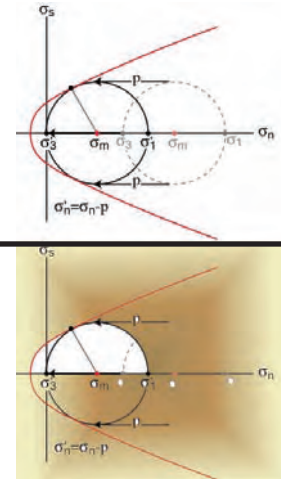


## 2. Fault mechanics: some basic aspects



The behavior of rocks in the shallow crust (fig. 7) has been extensively investigated with rock mechanics laboratory experiments. The results of experiments on the failure of intact rocks are graphically expressed using Mohr diagrams that relate principal stresses acting on a rock volume to shear stresses acting on planes differently oriented within the body. In Mohr diagrams (figs. 8, 9, 10), the composite failure envelope for intact isotropic rock is constructed by merging the Griffith and

Coulomb criteria (JAEGER & COOK, 1979; SIBSON, 1998). Three failure modes of intact rock have been recognized (ENGELDER, 1999; SIBSON, 1998): tensional fracturing, transitional-tensional fracturing (also called in literature extensional-shear fracturing, e.g., SIBSON, 1998) and compressional failure (also called in literature compressional shear failure, e.g., SIBSON, 1998). The first two failure modes occur when the effective minimum stress is tensional and are generally considered to occur only for fluid pressures greater than lithostatic in thrust regimes or at shallow depths in normal fault regions (SIBSON, 1998). Tensional fracturing mainly controls the development of extensional fractures in rocks, whereas the compressional failure applies to development of faults and is governed by the Coulomb fracture criterion:  $\tau = C + \sigma\mu$  where  $\tau$  is the shear stress,  $C$  is the cohesive shear stress,  $\sigma$  is the normal stress and  $\mu$  is the angle of rock internal friction. The slope of the Coulomb envelope is controlled by the coefficient of internal friction of rocks involved in the deformation. Laboratory strength tests on a wide range of rock types have shown that



Fig. 7 - Plumose structure on a fracture in lavas at Colcuc (Dolomites). Note on the left the center of nucleation of the fracture.

the internal friction coefficient ranges between 0.5 and 1.0 (e.g., JAEGER & COOK, 1979). It has been shown that in isotropic bodies (quite a rare situation in the Earth's crust), thrust faults are most likely to form from

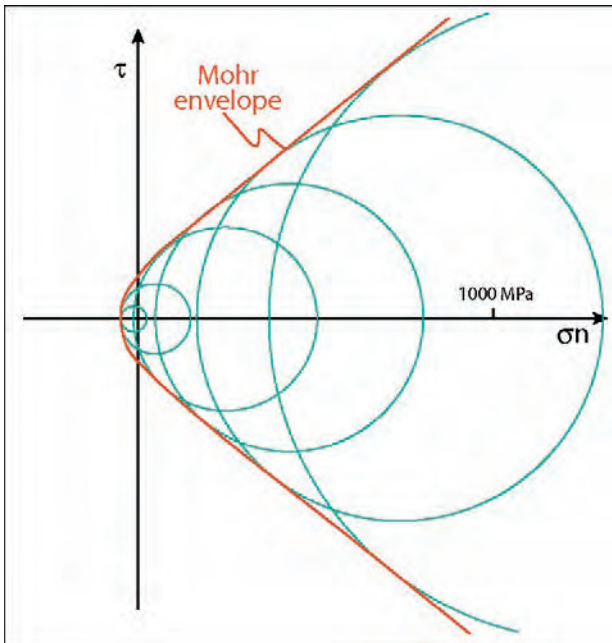


Fig. 8 - Mohr diagram showing the state of effective stress at failure for various experiments (varying the confining and the axial load) with intact Fredrick Diabase. Each circle represents the state of stress at failure at a different mean stress ( $(\sigma_1 + \sigma_2 + \sigma_3)/3$ ). The locus of stress states that bounds the field of stable and unstable stresses is called the Mohr envelope (after SUPPE, 1985).

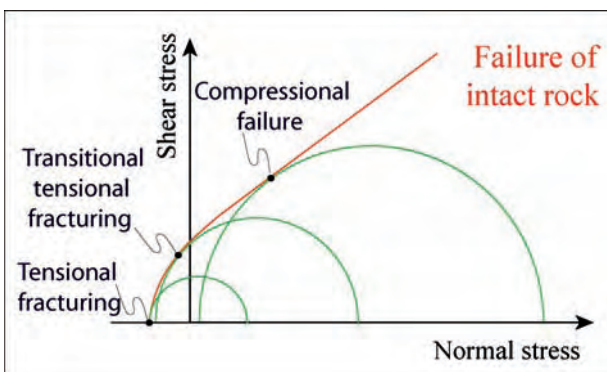


Fig. 9 - Generic Mohr diagram showing a composite Griffith-Coulomb failure envelope for intact rocks. The three shown critical stress circles represent different failure modes: tensional fracturing, transitional-tensional fracturing (also called in literature extensional-shear fracturing) and compressional failure (also called in literature compressional shear failure).

intact rocks at an angle of about  $30^\circ$  to  $\sigma_1$  (fig. 11). ANDERSON (1905) used the Coulomb-Mohr theory to explain conjugate faults and the different mean dip of the various types of faults. The Anderson's theory applies close to the Earth's surface, where one of the principal stresses needs to be vertical and the two remaining horizontal (due to the fact that, being a solid-air interface, the Earth's surface cannot sustain shear stresses). The main compressional stress  $\sigma_1$  is vertical in extensional regimes and consequently normal faults normally develop with high (dip around  $60^\circ$ ) angle, whereas it is horizontal in contractional areas and thrust faults consequently develop with low angle (around  $30^\circ$ ). In strike slip settings  $\sigma_2$  is vertical and strike-slip faults are mainly subvertical. Important classes of faults that appear to contradict the Anderson's theory are low angle normal faults and high angle reverse faults.

Fluid (e.g., water and hydrocarbons) pressure affects significantly the mechanics of faulting (fig. 12). High fluid pressures (caused by rapid burial of impermeable strata, thermal water pressuring and dehydration reactions occurring during burial and metamorphism) reduce drastically the stress needed to generate rock fracturing and formation of faults, since it supports part of the normal stress that would otherwise act across rock grain boundaries. The normal stress is then reduced to a lower effective normal stress. Extremely high pore fluid pressure will promote hydrofracturing (a process normally induced in oil wells to increase the permeability of reservoir rocks) and vein development. Normally, faults are associated with hydrothermal extensional vein systems (fig. 13). Veins are mainly horizontal when associated to thrust faults and subvertical for normal faults.

Reactivation of existing faults accounts for most of the deformation within the frictional seismogenic crust (fig. 14). In Mohr diagrams, the frictional failure envelope follows the

linear Amonton's law and, for faults characterised by cohesive strength, is a form of the Coulomb envelope (fig. 15). The slope of the Amonton envelope is controlled by the sliding coefficient of friction of the fault, which has been shown to have typical values as high as 0.85 in the shallow crust (BYERLEE, 1978). The frictional resistance along pre-existing planes is expressed by the Byerlee's law:  $\tau = 0.85\sigma$ . The Byerlee's law is broadly litho-logy-insensitive. Fault surfaces that contain a layer of gouge also obey Byerlee's law and display a frictional behavior similar to clean rock surfaces involving either strong and weak lithologies. The only silicatic minerals that display significant lower friction than Byerlee's law are montmorillonite, vermiculite and illite. Other platy minerals (e.g., chlorite, kaolinite and serpentine) display normal frictional properties.

The existence of near optimally oriented faults (at an angle close to  $30^\circ$  from  $\sigma_1$ ) normally inhibits the development of new planes by brittle failure. As the orientation of existing faults becomes less favourable, reactivation occurs for increasingly higher effective stresses until the angle of frictional lockup is reached and Coulomb mode rupture is expected to occur (HANDIN, 1969). For example, in compressional settings characterised by pre-existing normal faults unfavourably oriented

with respect to  $\sigma_1$  pre-existing normal faults are expected to remain unsheared and new fault planes may develop. Domino tilting of faults in extensional and compressional areas may progressively rotate the active fault plane so that they may acquire an unfavourable orientation for re-shearing, may lock-up and be abandoned. Further deformation will require the nucleation of new, favourably oriented faults.

Most of the theory on fault mechanics is based on the assumption of isotropic rock. This assumption is largely inconsistent with the observations both in sedimentary and basement rocks, where stratification, schistosity and other metamorphic and igneous foliations occur. In strongly anisotropic rocks, the orientation of the forming fractures is generally influenced by the foliation. Only in case of planes of anisotropy nearly perpendicular to the  $\sigma_1$  direction, unisotropy is unimportant in localizing fractures (fig. 16).

The displacement distribution along normal and thrust faults is maximum at the fault center and dies out to the fault margins. The thickness of the fault gouge is direct function of total slip along the surface (fig. 17).

The mechanics of thrust faulting has been the subject of animated discussion since when large thrust sheets were recognized. The mechanical problem is that thrust sheets are

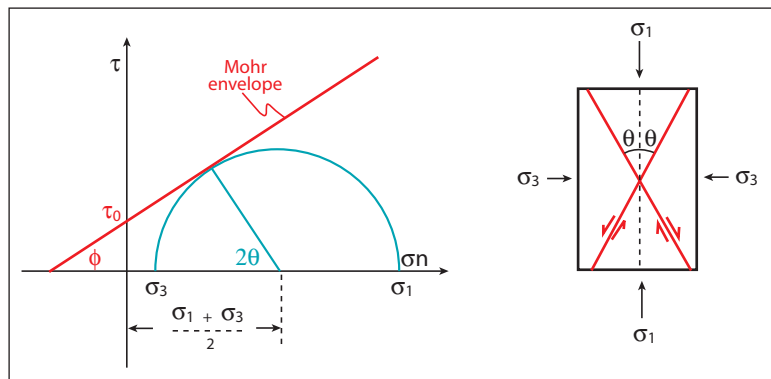


Fig. 10 - Mohr-Coulomb failure criterion for isotropic intact rocks (left panel). The point of tangency of the Mohr circle represents the state of stress on the plane which is at an angle  $\Theta$  from the  $\sigma_1$  axis of the right panel.

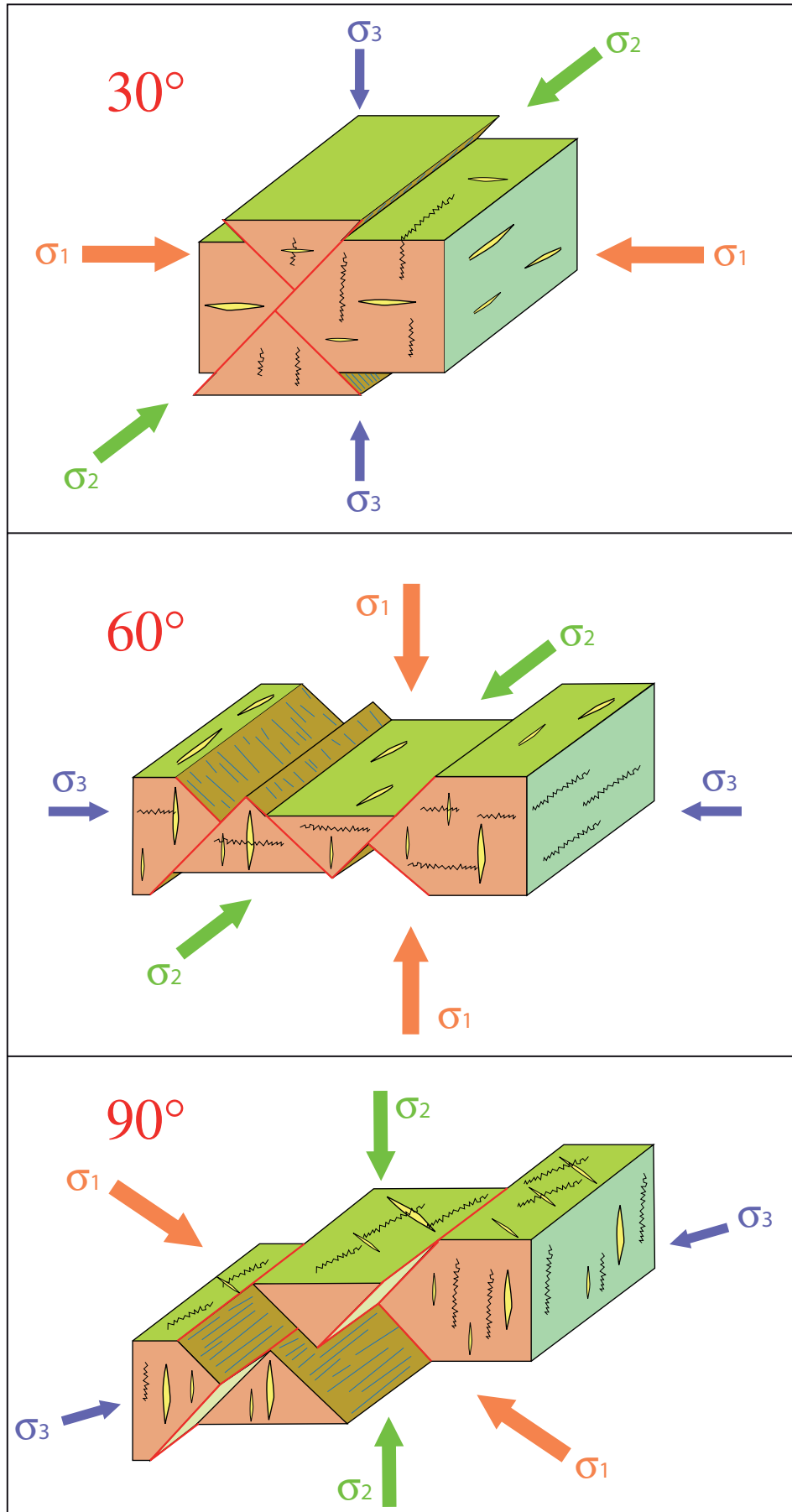


Fig. 11 - Anderson's theory of faulting. The structures associated to fault planes (i.e., stylolites, extensional fractures and veins) are also shown.

very thin relative to their apparent frictional resistance. When thrust faulting is reduced to the elementary physics problem of pushing a rigid block over a rigid base, the force with which the thin sheet has to be pushed determines stresses that are even an order of magnitude larger than the yield stress of common rocks.

Several solutions were proposed to solve this enigma: 1) the basal resistance is not expressed by Coulomb friction but is viscous or plastic (i.e., lower than expected); 2) thrusts are not pushed from behind but slide along dipping planes; 3) fluid pressures may lower the frictional resistance along the basal surface and enhance thrusting; 4) mountain belts are plastic masses that flow outward under their own

weight; 5) mountain belts may be modelled as critical tapers, similar to the deformed wedges of snow or sand developing in front of a bulldozer.

At present the two more accepted explanations invoke the role of fluids and the critical taper behavior of thrust faults. Two lines of evidence suggest that fluid pressures play a significant role: 1) pumping of fluids in reservoirs near active faults produces small earthquakes; 2) fluid pressure measurements in active regions show that major thrusts are confined to overpressured rock volumes.

The critical taper theory suggests that fold-and-thrust belts and accretionary prisms are first characterised by internal deformation and development of a topographic gradient

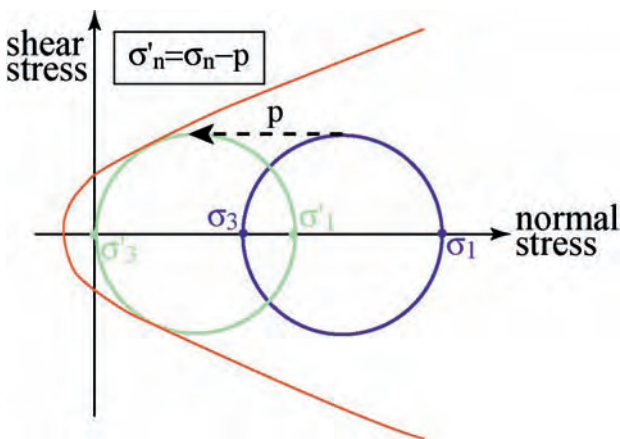


Fig. 12 - Mohr stress diagram showing the effects of pore fluid pressure on the state of stress of a rock volume. An increase of pore fluid pressure  $p$  lowers the principal stresses acting on the body and shifts the corresponding Mohr circle to the left. In this example, the dry rock is stable (i.e., it does not fracture since it does not reach the Mohr envelope) whereas the same rock volume, when subject to fluid pressure, may be unstable, i.e. characterised by a Mohr circle tangent to the Mohr envelope.  $\sigma_n$  is the normal stress.

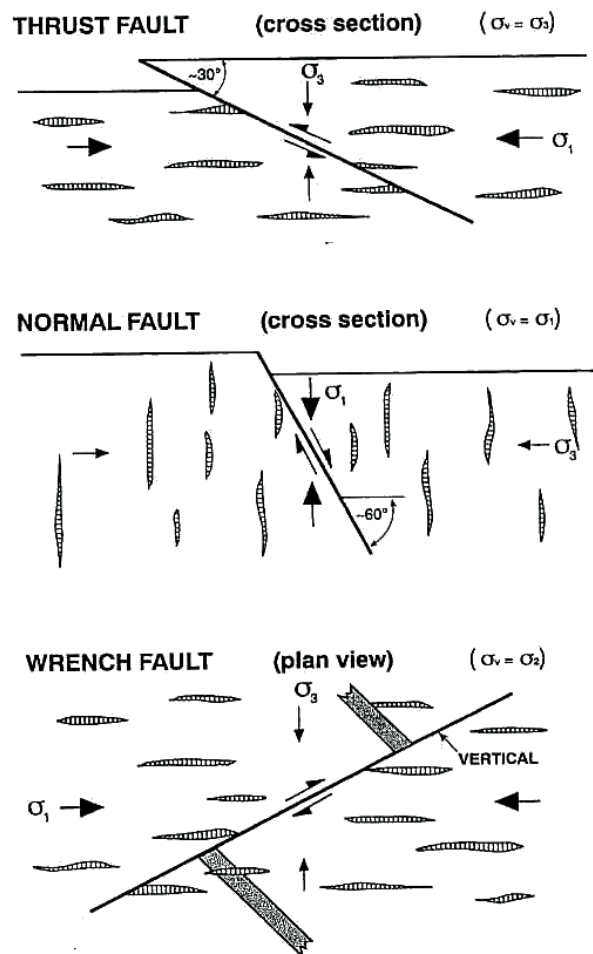


Fig. 13 - Hydrothermal extensional vein systems associated to Anderson style fault systems (after SIBSON, 1990).

without sliding on the basal surface (or decollement) and developing a wedge shape (figs. 18, 19, 20). Only when the wedge attains its critical taper (given by the sum of  $\alpha$ , the surface slope dip, and  $\beta$ , the basal decollement dip), the belt starts sliding stably, continuing to growth at constant taper as additional material

enters the belt at the front. If, at a specific point, the critical taper of a wedge is less than the critical value (because of erosion, for example), then the material will deform in more internal sectors (for example with the development of out of sequence thrusts) until the critical value is once again attained. At this

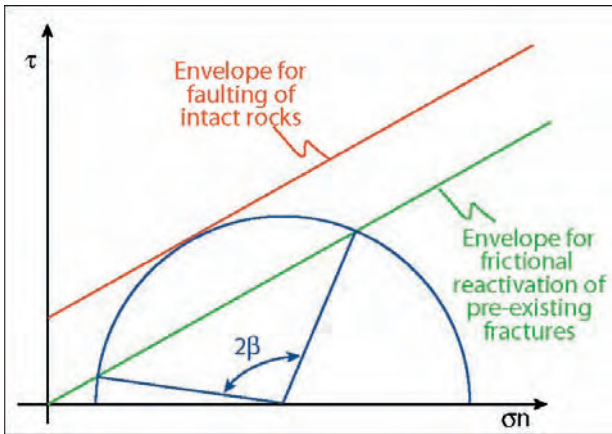


Fig. 14 - Fracturing of intact rocks vs. frictional reactivation of pre-existing faults. The frictional reactivation envelope for pre-existing faults is lower than that for faulting of intact rocks. The stress required for frictional sliding along pre-existing fractures is significantly less than the fracture strength. Two circles for fracture of intact rock (i.e., tangent to the Mohr envelope labeled as "faulting of intact rock") are shown. For the stress distributions associated to the two circles, frictional sliding on pre-existing fractures should anticipate the development of a new fault plane provided that such fractures have orientations comprised in the  $2\beta$  angles shown in figure

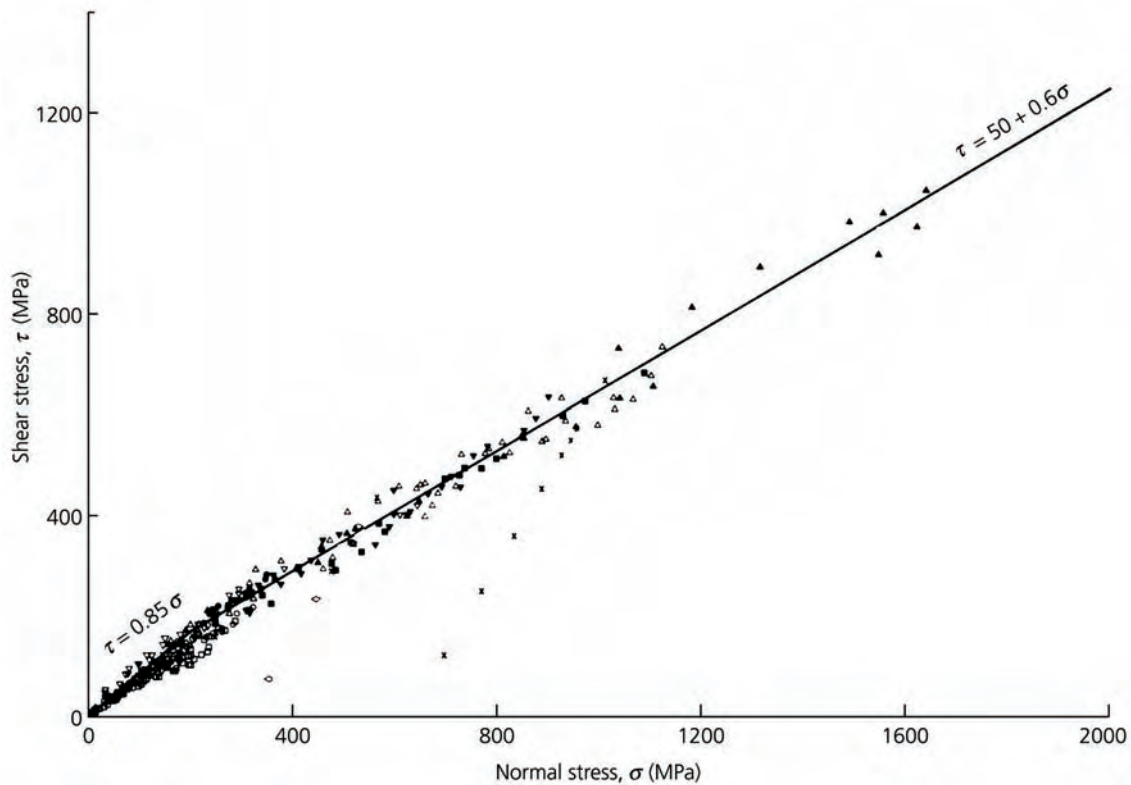


Fig. 15 - Measurements of maximum friction in sandstone, limestone and graywacke. The frictional resistance along pre-existing planes is expressed by the Byerlee's law:  $\tau=0.85\sigma$ . Notice that, in the shallow crust (for lithostatic pressure lower than 0.2 GPa) the cohesion is null. The Byerlee's law is broadly lithology-insensitive and is valid for fault surfaces involving either strong and weak lithologies that may contain a layer of gouge as well. The only silicatic minerals that display significant lower friction than Byerlee's law are montmorillonite, vermiculite and illite (after BYERLEE, 1978).

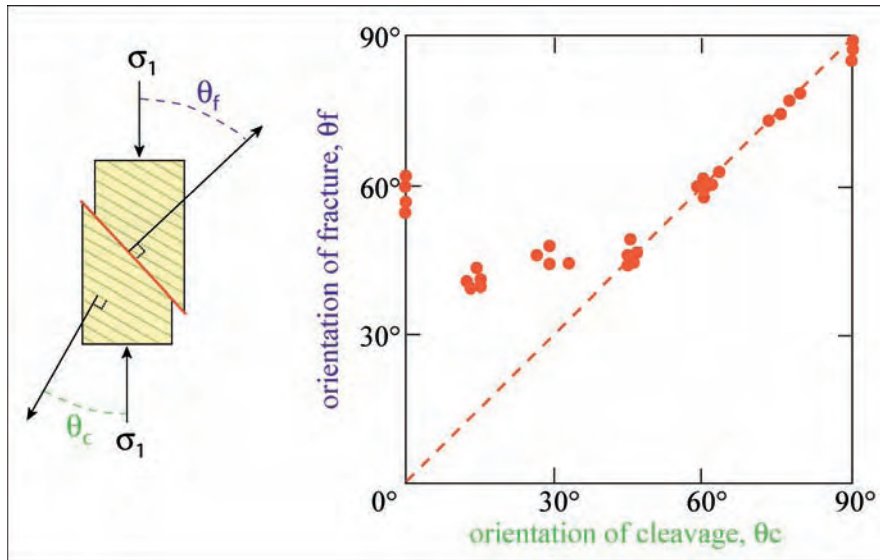


Fig. 16 - Fracturing in anisotropic rocks. The effect of the orientation of the plane of slaty cleavage on a fracture orientation is investigated in compressive fracture experiments on Martinsburg Slate. The orientation of the forming fractures is generally influenced by the foliation. For inclination of the slaty cleavage to the  $\sigma_1$  of as much as  $45^\circ$ , the fracture always lay parallel to the cleavage. Only in cases for which the plane of anisotropy is nearly perpendicular to the  $\sigma_1$  direction, anisotropy is unimportant in localizing fractures (after SUPPE, 1985).

point migration of the belt and accretion of material at the thrust front will start again. Typical values of surface slope dips are between  $1^\circ$  and  $10^\circ$ , whereas decollement dips

may be as high as ca.  $20^\circ$ . When the basal decollement runs within low-friction or ductile rocks, then the surface slope becomes about horizontal and plateaus develop.

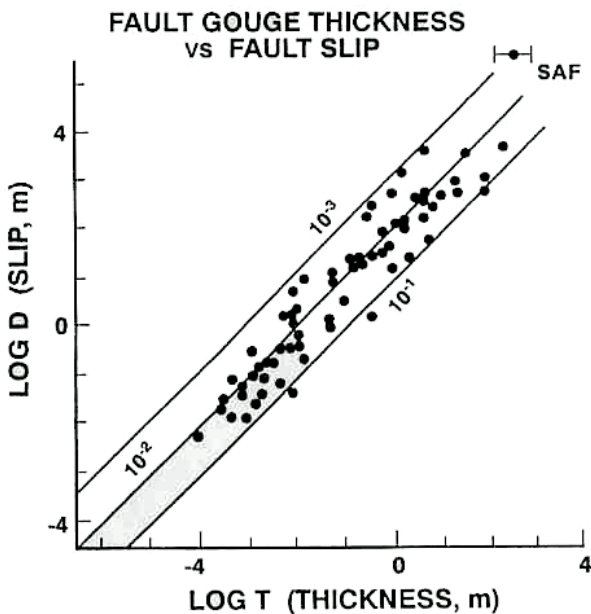


Fig. 17 - Fault gouge thickness ( $T$ ) vs. total slip ( $D$ ) for faults mainly developed in crystalline rocks (after SCHOLZ, 1990).

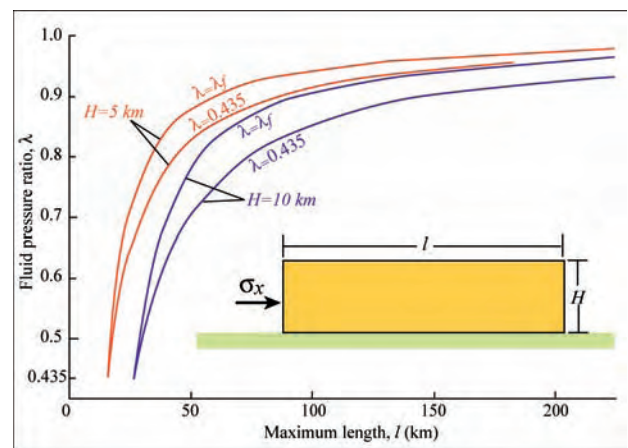


Fig. 18 - Maximum length ( $l$ ), as a function of fluid pressure ratio ( $\lambda = P_f/P_l$ , where  $P_f$  is the fluid pressure and  $P_l$  is the lithostatic pressure) of a rectangular thrust sheet that can be pushed along a horizontal decollement without fracturing.  $\lambda$  is the fluid pressure within the thrust sheet and  $\lambda f$  is the fluid pressure along the fault (after SUPPE, 1985).

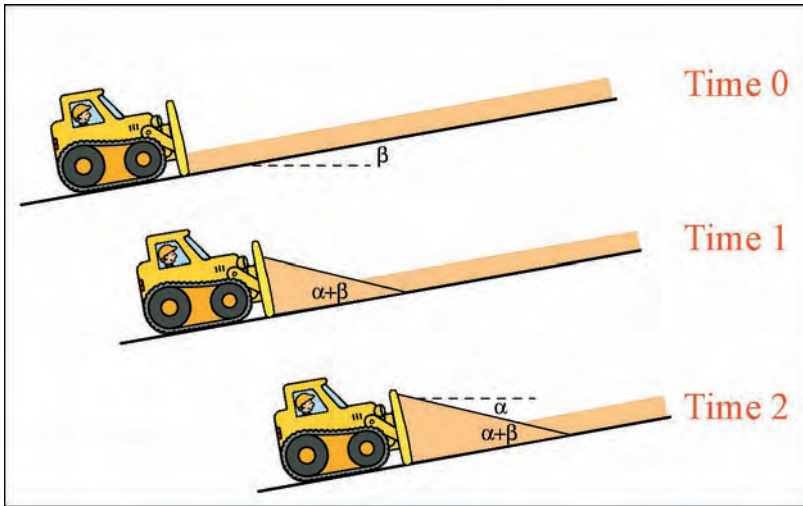


Fig. 19 - Contractional belts are normally modelled as purely brittle critical tapers deforming internally and spreading under the action of body (gravity) and surface (tectonic) forces (upper panel). These models successfully reproduce large scale topographic signatures of several wedge-shaped deformed regions (accretionary wedges) overlying a basal décollement. Surface slope and basal decollement dips predicted for submarine and subaerial accretionary wedges worldwide are shown in the bottom panel (after DAVIS *et alii* 1983).

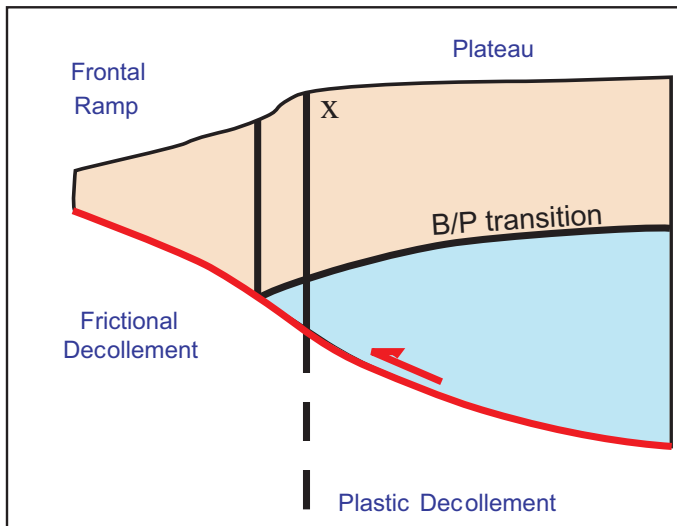
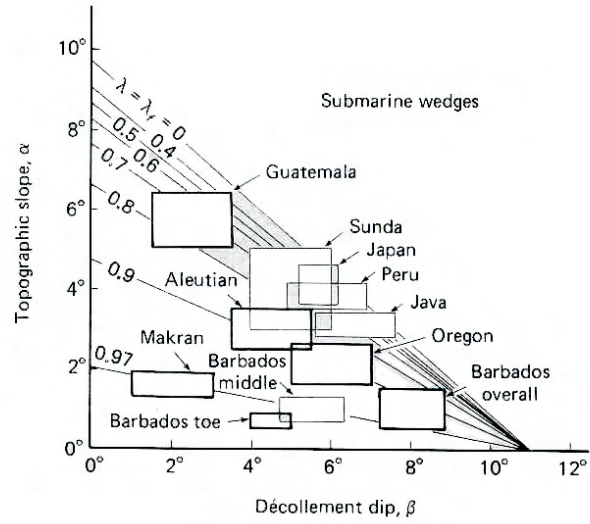
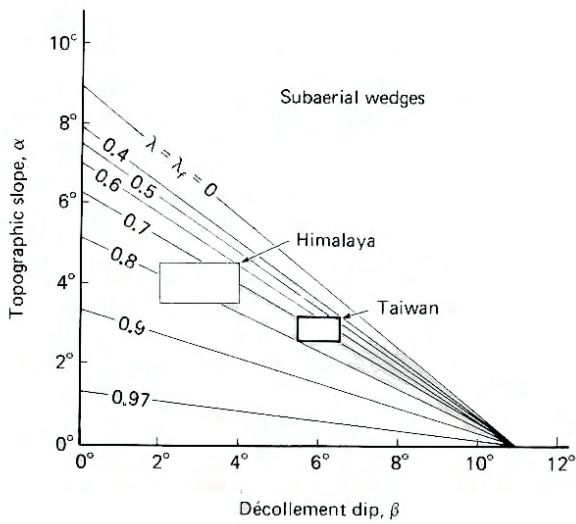


Fig. 20 - The topographic features of mountain belts are controlled by the rheological behavior of the basal decollement. Low-angle surface slopes, typical of frontal sectors of wedges deforming with a purely brittle (frictional) behavior, are interrupted by relatively steeper slopes, where the lowermost part of the wedge (wedge base) crosses the brittle/plastic transition and starts creeping while the basal décollement, deforming at higher strain rates, still behaves frictionally. Further to the rear, where both the wedge base and the décollement are plastic, the surface slope flattens (plateau). After CARMINATI & SILETTO (1997).